

Performance Study of Charcoal-based Radon Reduction Systems for Ultraclean Rare Event Detectors

M. Arthurs^a, D.Q. Huang^a, C. Amarasinghe^a, E. H. Miller^b and W. Lorenzon^a *

^a*Randall Laboratory of Physics, University of Michigan, Ann Arbor, Michigan 48109-1040, USA*

^b*SLAC National Accelerator Laboratory, Menlo Park, California 94025-7015, USA*

E-mail: lorenzon@umich.edu

ABSTRACT: The continuous emanation of radon due to trace amounts of uranium and thorium in detector materials introduces radon to the active detection volume of low-background rare event search detectors. ^{222}Rn produces a particularly problematic background in the physics region of interest by the “naked” beta decay of its ^{214}Pb daughter nucleus. While charcoal-based adsorption traps are expected to be effective for radon reduction in auxiliary circulation loops that service the warm components of current ton-scale detectors at slow flow rates ($0.5 - 2$ SLPM), radon reduction in the entire circulation loop at high flow rates ($\mathcal{O}(100\text{s SLPM})$) is necessary to reach high sensitivity in future generation experiments. In this article we explore radon dynamics with a charcoal-based radon reduction system in the main circulation loop of time projection chamber detectors. We find that even for perfect radon traps, circulation speeds of $2,000$ SLPM are needed to reduce radon concentration in a 10 ton detector by 90%. This is faster by a factor of four than the highest circulation speeds currently achieved in dark matter detectors. We further find that the effectiveness of vacuum swing adsorption systems, which have been employed very successfully at reducing atmospheric radon levels in clean-rooms, is limited by the intrinsic radon activity of the charcoal adsorbent in ultra-low radon environments. Adsorbents with about 20 times lower intrinsic radon activity than in currently available activated charcoals would be necessary to build effective vacuum swing adsorption systems operated at room temperature for rare event search experiments. If such VSA systems are cooled to about 190 K , this factor drops from 20 to about 3. This may be in reach by the time future generation experiments can be realized.

KEYWORDS: Dark Matter detectors; Time Projection Chambers; Noble liquid detectors, Liquid xenon target.

*Corresponding author.

Contents

1. Introduction	1
2. Radon Dynamics in a TPC Dark Matter Detector	2
3. Performance of a Single-Trap RRS	5
4. Swing Adsorption for Radon Reduction	9
4.1 Feasibility of Swing Adsorption RRS for Xenon	10
4.1.1 Swing Adsorption RRS with Feedback Loop and zero Intrinsic Activity	11
4.1.2 Adding a cold single trap to the Feedback Loop	13
4.1.3 Swing Adsorption RRS with non-zero Intrinsic Activity	15
4.1.4 Operating a cold Swing Adsorption RRS	18
5. Conclusion	19
A. A closer look at the single-trap in the Feedback Loop	20
B. Considerations for the Feed Cycle Time in a Swing Adsorption RRS	21

1. Introduction

Radon is a radioactive noble gas that is re-supplied continuously from the decay chains of uranium and thorium present in practically every material of rare event detectors, and constitutes the dominant background source in many dark matter searches. Because radon is an inert gas, it dissolves in noble liquid detectors and cannot be removed with high temperature getters. Among the radon isotopes abundant in nature, ^{222}Rn ($\tau = 5.516$ days), a progeny of ^{238}U , is of particular concern. The beta decay of its daughter ^{214}Pb has a gammaless component (6% b.r.) directly to the ground state of ^{214}Bi . This “naked” beta decay can end up in the low-energy region of interest for dark matter searches, survive the nuclear recoil discrimination cut, and be indistinguishable from low-energy nuclear recoils of rare particle interactions in the active volume of the detector. Discriminating against such background events is very challenging in the analysis.

Hardware mitigation is necessary to reduce the continuously re-supplied radon background for ton scale and larger noble-liquid rare event searches, including dark matter direct-detection experiments. LZ¹ is one ton-scale dark matter experiment [1] that addresses this need by introducing an

¹For illustration purposes we will occasionally refer to the LZ experiment, which is an experiment with a detector mass of about 10 tons of LXe. Note, however, that the general arguments are not limited to one specific dark matter effort.

in-line radon reduction system (iRRS) in an auxiliary circulation loop [2]. XENONnT is a different ton-scale dark matter experiment that employs inline distillation columns to address this need [3]. The LZ iRRS, which is based on a *single* adsorption trap, takes in a small stream ($0.5 - 1$ SLPM) of radon-rich gaseous xenon from the warm regions of the xenon gas circulation system, and returns the radon-reduced xenon back to the main circulation loop. While it is expected to reduce an estimated $\mathcal{O}(20 \text{ mBq})$ radon burden from the warm regions to below 1 mBq, it does not have the capacity to purify the entire 10 tons of liquid xenon.

For radon reduction in the entire system, rather than in a few select areas, an iRRS in the main xenon circulation loop becomes necessary. This requires a larger trap (i.e. more adsorbent) to accommodate the much higher flow rates needed for purifying multi-ton dark matter detectors. As explored in Sec. 3, scaling up charcoal based *single-trap* radon reduction systems for multi-ton time projection chambers (TPCs) is impossible given the intrinsic radon emanation of currently-available charcoals, and impractical even if radon emanation were negligible.

Pressure swing adsorption (PSA) systems have been shown to be very effective at reducing atmospheric radon levels in clean-rooms [4]. PSA systems are commonly employed as *two-trap* systems where the main flow of the carrier gas is alternated between the two charcoal columns allowing one column to be filled while the other is purged. Pioneering the development of PSA technology for radon reduced clean rooms, vacuum swing adsorption (VSA) systems (where the purge is at pressures of $\mathcal{O}(10 \text{ mbar})$) have demonstrated radon reduction efficacy of 99.7% in air at flow rates as high as 2,000 SLPM [4–6]. Section 4 explores the effectiveness of a swing adsorption system suitable for noble liquid detectors that are operated at room temperature or cooled to almost noble liquid temperature. The figures and simulations in this work are available from a public Gitlab repository [7].

2. Radon Dynamics in a TPC Dark Matter Detector

A schematic diagram of radon dynamics in a TPC detector with a RRS in the main circulation path² is represented in Fig. 1. For a total radon emanation rate S in the detector, the rate of change of the number of radon atoms in the detector, N , is given by

$$\frac{dN}{dt} = -\lambda N - \Phi N + S + \gamma(\Phi N), \quad (2.1)$$

where $-\lambda N = dN_{\text{decay}}/dt$ is the radon decay rate in the TPC with decay constant $\lambda = 1/\tau$; $-\Phi N = dN_{\text{out}}/dt$ is the rate of radon atoms flowing out of the TPC set by the volume exchange time T of the entire detector mass, with $T = 1/\Phi$; and $\gamma(\Phi N)$ is the inflow of radon atoms that escape the RRS, with $\gamma = N_{\text{out}}/N_{\text{in}}$ being the fraction of radon atoms escaping the RRS. For simplicity we exclude radon sources within the circulation path.

²The main circulation path in a TPC detector refers to the gas circulation and purification system that is needed for TPC detectors to remove a) electronegative impurities, such as oxygen and water that limit the free electron lifetime and degrade the operation of the TPC, and b) radioactive noble gases. Purification from electronegative impurities is achieved with getters containing zirconium that are operated at high temperatures, typically near 600C. This requires noble liquids to be gasified before they can be introduced to the getters. Since radioactive noble gases cannot be removed with those getters, radioactive noble elements have to be removed with other means.

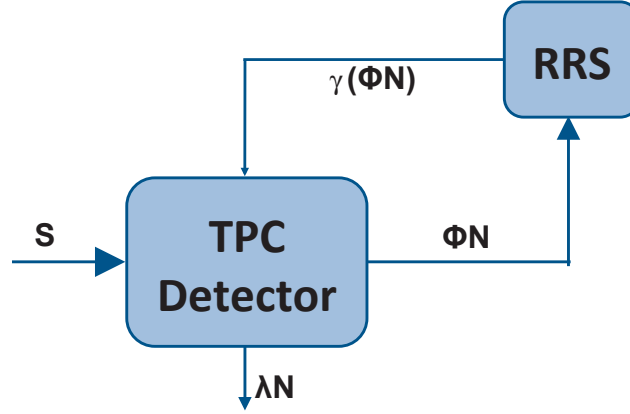


Figure 1. Schematic diagram of radon dynamics in the active volume of a dark matter detector (TPC) with a radon reduction system (RRS) in the main circulation path. Note that ΦN is the rate of radon atoms flowing out of the TPC; S is the radon activity in the detector; N is the number of radon atoms in the detector; and γ is the fraction of radon atoms escaping the RRS.

Rearranging Eq. (2.1) leads to

$$\frac{dN}{dt} = -(\lambda + \Phi(1 - \gamma))N + S = -\Lambda N + S, \quad (2.2)$$

which can be solved to find the total number of radon atoms

$$N(t) = -Ce^{-\Lambda t} + \frac{S}{\Lambda}, \quad (2.3)$$

where $\Lambda = \lambda + \Phi(1 - \gamma)$ is assumed to be constant. In Eq. (2.3), C is an integration constant defined by the initial conditions. Since we are interested in the number of radon atoms in the TPC when equilibrium is reached, we can take the limit $t \rightarrow \infty$ to obtain the steady state number of radon atoms

$$N_{ss} = \frac{S}{\Lambda} = \frac{S}{\lambda + \Phi(1 - \gamma)} = \frac{S}{\lambda + \Phi\epsilon_{RRS}}. \quad (2.4)$$

where $\epsilon_{RRS} = 1 - N_{out}/N_{in}$, defined as the efficacy of a RRS, is a parameter that refers to the effective performance of the trap. It encapsulates both the reduction of external radon introduced to the inlet of the trap, and radon emanation from the trap due to its intrinsic activity. It describes the net fraction of radon atoms removed by the trap, such that a fraction of 1 indicates a perfect trap, ie. no radon atoms emerge from the trap; a fraction of 0 indicates an ineffectual trap, ie. the same number of radon atoms enter and exit the trap; and a trap which adds more radon atoms than it removes will have a negative ϵ_{RRS} .

The number of radon atoms exiting the trap is given by

$$N_{out} = (1 - \eta)N_{in} + N_{trap}, \quad (2.5)$$

where η is the remanent fraction of the trap, which refers to the fraction of trapped inlet radon atoms, and N_{trap} is the contribution to the trap output due to radon emanation of the trap. Combining Eq. 2.5 with the definition of efficacy leads to

$$\epsilon_{RRS} = \eta - N_{trap}/N_{in}. \quad (2.6)$$

This will be explored in greater detail in Secs. 3 and 4.

If there is no circulation at all, there will be no radon reduction. This would result in the highest possible steady state radon count in the detector,

$$N_{max} = \frac{S}{\lambda}. \quad (2.7)$$

The fractional radon reduction with a RRS is expressed by the ratio of Eqs. (2.4) and (2.7), such that

$$\frac{N_{ss}}{N_{max}} = \frac{\frac{S}{\lambda + \epsilon_{RRS}\Phi}}{\frac{S}{\lambda}} = \frac{\lambda}{\lambda + \epsilon_{RRS}\Phi} = \frac{\frac{1}{\tau}}{\frac{1}{\tau} + \frac{\epsilon_{RRS}}{T}} = \frac{T}{\epsilon_{RRS}\tau + T}. \quad (2.8)$$

Hence, radon reduction efficacy with a RRS in the main circulation loop of the detector, defined as $\epsilon_{det} = 1 - N_{ss}/N_{max}$, is given by

$$\epsilon_{det} = 1 - \frac{N_{ss}}{N_{max}} = \frac{\tau}{\tau + T/\epsilon_{RRS}}. \quad (2.9)$$

For a perfect radon reduction system ($\epsilon_{RRS} = 1$), the highest achievable radon reduction efficacy becomes

$$(\epsilon_{det})_{max} = \frac{\tau}{\tau + T}. \quad (2.10)$$

This means that the maximum achievable radon reduction efficacy is ultimately limited by the volume exchange time of the detector.

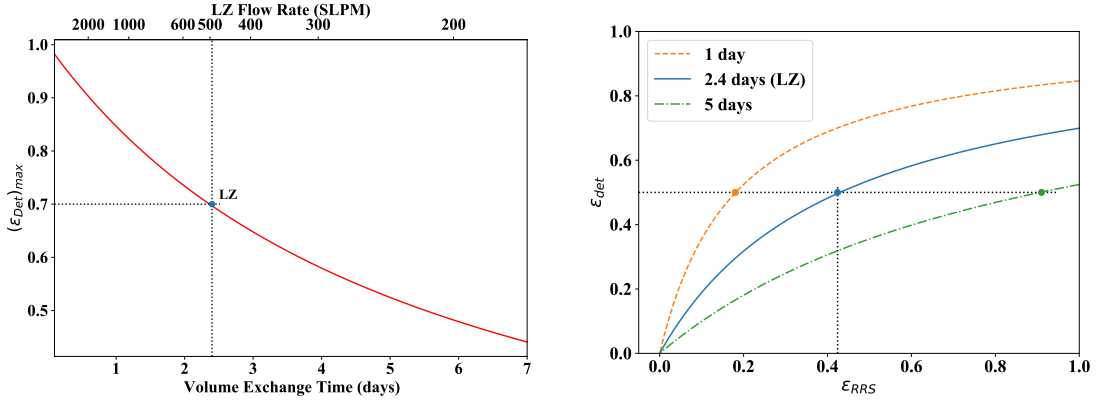


Figure 2. Left panel: Maximum achievable radon reduction efficacy with a perfect radon trap in the main circulation loop as a function of the volume exchange time of a TPC detector. The blue filled circle indicates the maximum efficacy for a volume exchange time of 2.4 days, which is explored in more detail in the right panel. Also shown is the maximum efficacy as a function of the circulation flow rate specifically for a 10-ton detector (top horizontal scale). The dotted black lines indicate the best radon reduction efficacy achievable for the conditions at LZ. Right panel: Radon reduction efficacy achievable in a detector as a function of RRS efficacy for three different volume exchange times. The horizontal dotted black line indicates the conditions needed to achieve a factor of two radon reduction in the detector.

The left panel of Fig. 2 shows the maximum achievable radon reduction efficacy in a detector as a function of volume exchange time with a perfect radon reduction system in the main circulation path. Also shown in the figure is the maximum achievable radon reduction efficacy as a function of

carrier gas circulation flow rate specifically for a 10-ton detector, such as in LZ. For that detector, with its $F = 500 \text{ SLPM}$ carrier gas circulation flow rate resulting in a volume exchange time³ of about $T = 2.4$ days, and given the radon lifetime of $\tau = 5.516$ days, at most a 70% radon reduction efficacy (i.e. a radon reduction factor of 3.3) can be achieved. In order to reach radon reduction close to 90% in LZ, flow rates of over 2,000 SLPM are necessary. For such high flow rates it is very challenging if not impossible with current technology to use high-temperature getters for gas purification (from electronegative impurities). Purification in the liquid phase using getters, operated at cryogenic temperatures, would have to be employed similar to what has been done in very large argon TPC experiments such as ICARUS [8].

The right panel of Fig. 2 shows that for detectors with imperfect RRSs, the faster the volume exchange time, the lower the requirements on the RRS to achieve a certain reduction efficacy. If we declare that a successful RRS has to provide at least a factor of two radon reduction (ie. $\epsilon_{det} = 0.5$), volume exchange times of at most 5.5 days have to be achieved with a perfect RRS (shown in left panel). If shorter volume exchange times can be achieved, demands on the RRS can be significantly reduced (shown in the right panel). For the conditions at LZ, a RRS with a 42% efficacy is sufficient to reach a 50% efficacy in the detector.

3. Performance of a Single-Trap RRS

Radon reduction in the single-trap RRS approach is accomplished by maintaining radon breakthrough times that are long enough that the vast majority of the radon atoms entering the trap decay, while the carrier gas quickly traverses the trap. The breakthrough time of a radon atom in a charcoal trap, t_b , defined by the chromatographic plate adsorption model, is given by Ref. [4] as

$$t_b = \frac{mk_a}{f}, \quad (3.1)$$

where m is the charcoal mass, k_a is the dynamic adsorption coefficient of radon on charcoal in a carrier gas, and f is the volumetric flow rate of the carrier gas. This is an example of gas chromatography where one takes advantage of the different propagation speeds for radon and the carrier gas in the charcoal trap. The propagation speeds can vary by several orders of magnitude, particularly at cryogenic temperatures, where a ratio of $v_{Xe}/v_{Rn} = 1,000$ has been reported [9]. If the trap is large enough, so that radon needs a few lifetimes to reemerge on the other side of the trap, the overall radon concentration in the carrier gas is reduced accordingly.

For an ideal trap, i.e. a trap with negligible intrinsic activity, with a breakthrough time t_b , radon reduction is given by an exponential decay law as

$$N_{out} = N_{in} e^{-\frac{t_b}{\tau}} = N_{in} e^{-\frac{mk_a}{\tau f}} = N_{in} e^{-\frac{m}{\mu}}, \quad (3.2)$$

where N_{in} is the number of radon atoms that enter the trap and N_{out} is the number of radon atoms that emerge from the trap, and $\mu = f\tau/k_a$ represents the characteristic mass of the trap, which is the mass of charcoal, at a given flow rate, needed to reduce radon activity by a factor of e .

³The volume exchange time is given by $T = M/(F\rho)$, where F is the carrier gas circulation flow rate, M is the total carrier gas mass, and ρ is the carrier gas density.

Equation (3.2) can also be expressed in terms of input activity A_{in} and output activity A_{out} , since $A = N/\tau$, so that

$$A_{out} = A_{in} e^{-\frac{t_b}{\tau}} = A_{in} e^{-\frac{mk_a}{\tau f}} = A_{in} e^{-\frac{m}{\mu}}. \quad (3.3)$$

For charcoals with the same adsorption properties as that used in the LZ iRRS [2] ($k_a = 500 \text{ l/kg}$) at 295 K, and $k_a = 3,000 \text{ l/kg}$ at 195 K) the amount necessary for an ideal trap to achieve 90% efficacy as a function of the circulation flow rate of the carrier gas is shown in Fig. 3.

The figure demonstrates that for the 500 SLPM carrier gas circulation flow rate at LZ, it would take about 3,000 kg of charcoal at 190 K or 20,000 kg at 295 K to achieve a 90% efficacy. A 3,000 kg cold trap of charcoal with a density of about 0.6 g/cm^3 would occupy a volume of roughly 5 m^3 , and adsorb almost 5,000 kg of xenon [2]. Thus, scaling of single-traps to sustain the high flow rates needed for multi-ton dark matter experiments is not a viable option, not even for ideal traps.

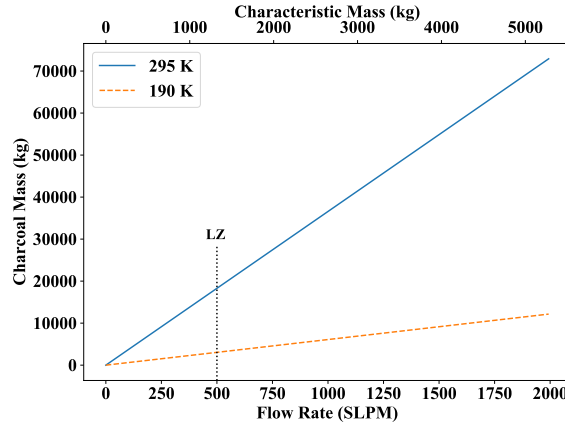


Figure 3. The amount of charcoal needed for 90% efficacy as a function of carrier gas flow rate for a single-trap RRS with zero intrinsic radon activity. The orange dashed line is at 190 K ($k_a = 3,000 \text{ l/kg}$), and the blue solid line is at room temperature, 295 K ($k_a = 500 \text{ l/kg}$). The dotted black line indicates the 500 SLPM carrier gas circulation flow rate in LZ.

For a realistic trap, charcoal has intrinsic activity that contributes radon atoms to the output of the trap. Intrinsic activity of a charcoal is typically given by its specific activity s_o in units of mBq/kg . For a charcoal trap of mass m with specific activity s_o , the total radon activity of the trap will be ms_o (i.e. the number of radon atoms emanating from the total charcoal mass per second). Note that not all of the emanated radon atoms escape the trap — some of them decay in the trap. For a charcoal trap of a mass M ($M \propto v_{Rn} t_b$), assuming uniform radon emanation over the entire trap, the radon activity of a charcoal slice with length dm between m and $m + dm$ can be expressed as

$$s_o dm = \frac{A_{em}}{M} dm = A_{em} \frac{dm}{M} = A_{em} \frac{v_{Rn} dt}{v_{Rn} t_b} = A_{em} \frac{dt}{t_b}, \quad (3.4)$$

where $A_{em} = s_o M$ is the total activity of a charcoal with specific activity s_o and mass M , and dt is given by $dt = dm/v_{Rn}$. The radon contribution at the output of the trap from a such infinitesimal slice is given by

$$dA_{trap} = \frac{A_{em}}{t_b} e^{-\frac{t}{\tau}} dt. \quad (3.5)$$

Integrating Eq. 3.5 over the trap breakthrough time gives the total radon contribution of the trap,

$$A_{trap} = \frac{s_o m}{t_b} \int_0^{t_b} e^{-\frac{t}{\tau}} dt = s_o m \frac{\tau}{t_b} \left(1 - e^{-\frac{t_b}{\tau}}\right) = s_o f \frac{\tau}{k_a} \left(1 - e^{-\frac{mk_a}{\tau f}}\right). \quad (3.6)$$

Combining Eqs. (3.3) and (3.6), the activity at the output of a single charcoal trap can be expressed as

$$A_{out} = A_{in} e^{-\frac{mk_a}{f\tau}} + s_o f \frac{\tau}{k_a} \left(1 - e^{-\frac{mk_a}{f\tau}}\right). \quad (3.7a)$$

This can be rewritten as

$$A_{out} = A_{in} e^{-\frac{m}{\mu}} + s_o \mu \left(1 - e^{-\frac{m}{\mu}}\right). \quad (3.7b)$$

Note that for sufficiently large traps, where $m \gg \mu$, the lowest achievable radon activity at the output of the trap is given by $A_{out} \approx s_o \mu$, and thus depends on the specific activity but not on the total mass of the charcoal.

The performance of a single-trap RRS is now explored in terms of RRS efficacy, which encapsulates both, the reduction of the inlet activity, as well as the contribution from the intrinsic activity of the charcoal. The efficacy of the such a trap, given by $\varepsilon = 1 - A_{out}/A_{in}$, can be expressed in terms of Eq. (3.7b), as

$$\varepsilon = 1 - A_{out}/A_{in} = 1 - e^{-\frac{m}{\mu}} - \frac{s_o \mu}{A_{in}} \left(1 - e^{-\frac{m}{\mu}}\right) = \left[1 - \frac{s_o \mu}{A_{in}}\right] \left(1 - e^{-\frac{m}{\mu}}\right). \quad (3.8)$$

It increases with increasing input radon activity. This makes the technique particularly well-suited for radon reduction from radon-rich environments.

The relevant parameter for the efficacy of a single-trap RRS is the ratio of the specific activity of the charcoal and the input radon activity, (s_o/A_{in}) . Together with the characteristic mass of the charcoal, it determines the maximal efficacy of a trap in the limit of $m \rightarrow \infty$ as

$$\varepsilon_{max} = 1 - \frac{s_o}{A_{in}} \mu = 1 - \left(\frac{s_o}{A_{in}}\right) \left(\frac{f\tau}{k_a}\right) = 1 - \frac{f}{f_{critical}}, \quad (3.9)$$

where $f_{critical} = (A_{in}/s_o)(k_a/\tau)$ is the critical flow rate of the carrier gas for a given single-trap condition (A_{in} , s_o , and k_a). Note that at the critical flow rate the efficacy of the trap becomes zero, and above it the trap becomes harmful. In order to design an effective single-trap it is necessary to chose a charcoal with high adsorptive properties (large k_a) and low intrinsic activity (small s_o), which translates to maximizing the critical flow rate of a trap.

Figure 4 explores the dependence of the single-trap efficacy on the flow rate for various charcoal masses. The flow rate is shown in units of critical flow rate, and the mass is given in units of characteristic charcoal mass of the trap. The figure shows that independent of charcoal mass, carrier gas flow rates of about an order of magnitude lower than the critical flow rate are necessary to reach maximal efficacy. At the critical flow rate, trap efficacy becomes zero independent of charcoal mass.

Figure 5 shows the single-trap efficacy as a function of trap mass for various flow rates of the carrier gas. The mass is given in units of characteristic charcoal mass of the trap, and flow rate is shown in units of critical flow rate. For flow rates below the critical flow rate, the efficacy of the trap increases with increasing charcoal mass and rapidly approaches its maximal value, until it reaches a trap mass of $\mathcal{O}(4\mu)$, above which the increase in the efficacy is asymptotically small.

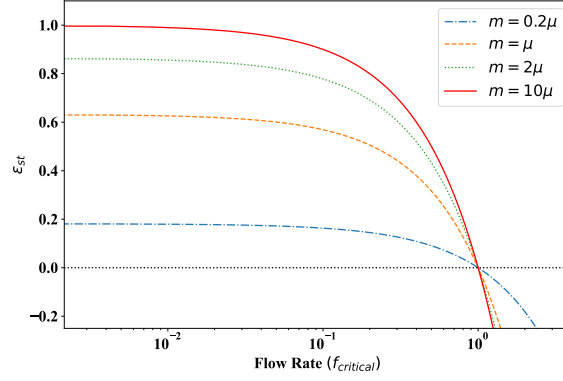


Figure 4. Efficacy of a single-trap RRS as a function of the flow rate in units of $f_{critical}$. At the critical flow rate, the efficacy becomes zero, independent of trap mass. Above it, the trap becomes harmful. The various curves represent different trap masses in units of the characteristic mass μ .

For illustration purposes, let us explore the trap efficacy for the LZ iRRS, shown in Fig. 6, which employs a synthetic charcoal called Saratech [2] in a single-trap approach. Saratech has a dynamic adsorption coefficient of 500 l/kg at room temperature that increases to $3,000\text{ l/kg}$ as the temperature falls to 190 K , which is slightly above the liquefaction temperature of xenon. Running the trap at cryogenic temperatures is advantageous, as it requires relatively small amounts of charcoal. The charcoal used in the LZ iRRS has an intrinsic activity of $\mathcal{O}(0.5\text{ mBq/kg})$ [2]. For an inlet radon activity of 20 mBq , the critical flow rate is $f_{critical} \approx 15\text{ SLPM}$. For flow rates below the critical flow rate, where radon contribution from the charcoal is smaller than radon reduction due to adsorption, a greater mass of charcoal results in a higher efficacy, as shown in Fig. 6. At the critical flow rate, shown as the inflection point in Fig. 6, the radon contribution from the charcoal compensates the reduction due to adsorption. Above the critical flow rate, the efficacy becomes negative indicating that the radon reduction system becomes harmful and introduces more radon atoms to the detector than it removes. Figure 6 also shows that at the relatively low flow rates of $0.5 - 1\text{ SLPM}$ at LZ, radon reduction efficacies of more than 90% can be achieved with a 10 kg (ie. 7.6μ) charcoal trap.

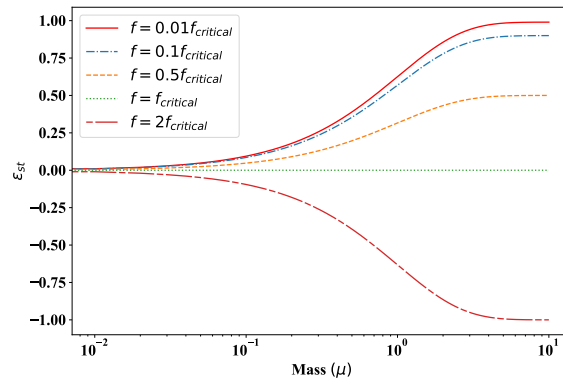


Figure 5. Efficacy of a single-trap RRS as a function of characteristic mass μ . For trap masses above about four characteristic masses (4μ), the increase in the efficacy is asymptotically small. The various colors represent different flow rates relative to the critical flow rate $f_{critical}$.

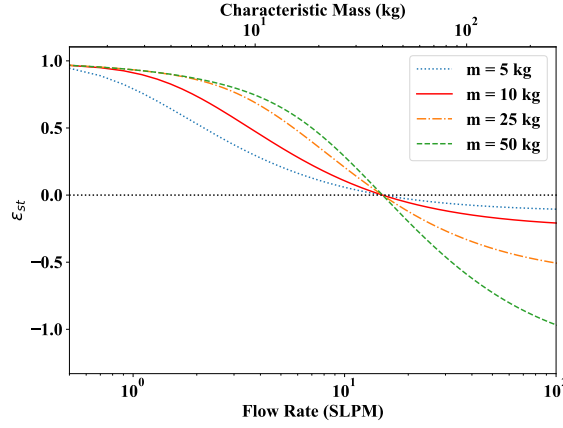


Figure 6. Efficacy of LZ iRRS (a 10kg charcoal single trap with dynamic adsorption coefficient of $k_a = 3,000\text{ l/kg}$ (at 190K), total inlet radon activity of $A_{in} = 20\text{ mBq}$) as a function of the flow rate of the carrier gas. The various curves represent efficacies for different masses of charcoal.

4. Swing Adsorption for Radon Reduction

Vacuum swing adsorption (VSA) systems have been developed for radon reduction in clean rooms for flow rates of order 1,000 SLPM. This is in contrast to single-trap radon reduction systems whose performance is set by the steady-state radon output, which limits the flow rate. VSA systems are systems commonly consisting of two charcoal columns where the flow direction of the carrier gas is periodically switched between the columns.

A schematic view of a VSA system for radon reduction in air is presented in Fig. 7. Ambient air is fed into column 1 (here the feed column) for a time much shorter than the time required for radon atoms to transit the column, while column 2 (here the purge column) is purged at low pressure with a small stream of radon-reduced air from the outlet end of column 1⁴ to flush the radon atoms out. As described in Section 4.1.3, the low pressure of the purge is necessary to obtain a regeneration cycle that is faster than the feed cycle. At the end of this cycle, column 2 has been regenerated and is ready to be fed with outside air, while column 1 has accumulated radon and is ready to be purged. With the beginning of the next cycle, the outside air is directed into column 2 (now the feed column), while column 1 (now the purge column) is purged. By the end of the second cycle, each column has gone through one feed and one purge cycle. The time required to complete these two cycles is typically called a swing-cycle period.

By switching a given flow between the two columns, each column may be much smaller than the column in a single-trap RRS. Unlike in single-trap reduction systems, where radon atoms are retained in the charcoal for many lifetimes, in a swing system they are flushed out of the system before most have a chance to decay. Additionally, unlike single-trap reduction systems, which are typically cooled down to cryogenic temperatures, VSA systems are shown to reach high efficacy even at room temperature. Over the past decade, VSA technology has been improved to reach radon reduction efficacy in air of greater than 99.9% [5, 6]. For an inlet radon activity of about 80 Bq/m^3 ,

⁴Typically about 10% of the radon-reduced air emerging from the outlet of the feed column is used for purging the radon-enhanced column while a vacuum pump maintains the column pressure at around 10 mbar.

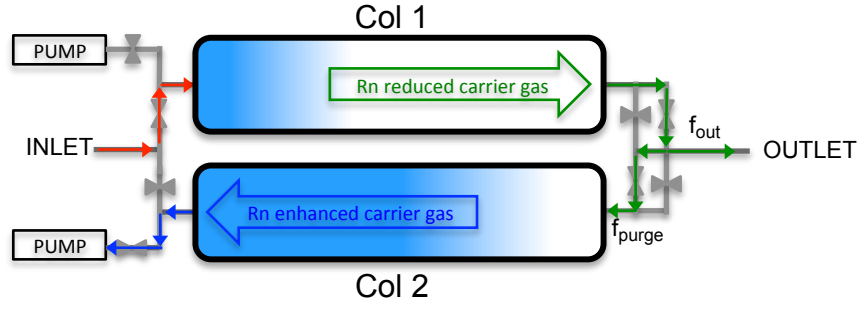


Figure 7. A schematic view of a VSA system for radon reduction in air. Flow of the input air is alternated between columns 1 and 2 to prevent radon escaping from the outlet ends of the columns. While one column is fed with air, the other is purged with a small stream of radon-reduced air. The shades of blue indicate the radon concentrations in the two columns, the red arrows indicate the flow of the input gas, the green arrows indicate the flow of the radon-reduced output gas, and blue arrows indicate the pump-out flow.

reduction factors of greater than 1,000 were achieved, reducing the clean room radon activity down below the sensitivity of the RAD7 measurement device, with an upper limit of 0.067 Bq/m^3 [6].

4.1 Feasibility of Swing Adsorption RRS for Xenon

Considering the great success of VSA systems for radon-reduced clean rooms, we will now explore the viability of such a system for full scale radon reduction in a rare-event TPC detector, taking into account some distinct differences.

Since the radon content introduced to a VSA system due to the intrinsic activity of charcoal is typically much smaller than that in atmospheric air, it is mostly ignored in VSA systems used for radon reduction in clean rooms. Conversely, in a liquid xenon dark matter detector with a radon content as low as 1 atom/kg of xenon, the introduction of a charcoal trap could very well introduce more radon than it removes. For simplicity, we will start with ignoring intrinsic activity (Sec. 4.1.1), and then study the impact of non-zero intrinsic activity on VSA systems (Sec. 4.1.3).

Furthermore, in contrast to air purification systems, where the purged air is released back into the atmosphere, xenon is expensive, and needs to be captured and returned to the purification system as shown schematically in Fig. 8. Therefore, rather than pumping and releasing the xenon gas into atmosphere, the radon-rich purge gas has to be returned to the inlet of the swing system. In such a system, the radon atoms become effectively trapped and accumulate in the feedback loop. Accumulation of radon atoms in the feedback loop continues until it is balanced by the decay of the radon atoms and steady state is reached. Note that such a system conveniently provides a mechanism for radon atoms to decay outside of the TPC detector.

Because of the cyclic nature of the swing system, its columns never reach steady state. The full modeling of the system is therefore more involved and must track radon concentrations throughout each column and propagate them over time. The exact behavior will depend strongly on the choice of charcoal [2], the geometry of the columns, the pumping speed of the system, and other system-dependent properties. While this system-dependent modeling is beyond the scope of this work, models prepared for other systems have shown that radon appearing at the VSA output is primarily due to the long diffusive tail of the radon front as it propagates through the charcoal [4]. Thus, the

remanent fraction of the VSA will depend on the elution curve of radon in the trap as well relative values of the cycle time and the trap breakthrough time. For simplicity, we fold this into a single constant remanent fraction for the feed column when modeling the performance of the VSA.

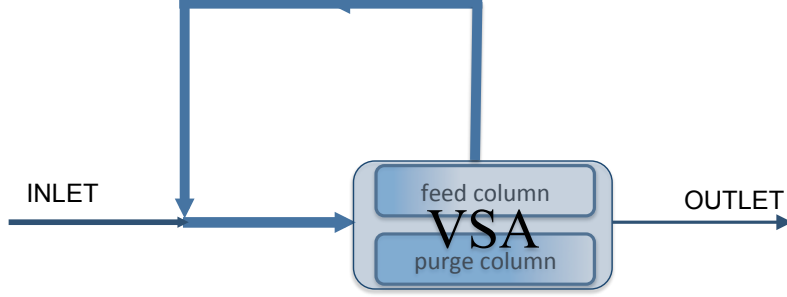


Figure 8. A schematic view of a VSA system with a feedback loop for radon reduction in xenon. Flow of the input xenon is alternated between the two columns, but unlike in a radon reduction system for air, where the purged air is released back into the atmosphere, the purged xenon is returned through a feedback loop to the inlet of the VSA.

4.1.1 Swing Adsorption RRS with Feedback Loop and zero Intrinsic Activity

In order to evaluate steady state conditions for a VSA system with a feedback loop, let us consider the dynamics of radon atoms in a single cycle. For simplicity, and to compare with radon reduction systems in clean rooms, we will start with ignoring intrinsic radon activity. Let us consider the situation where some radon atoms entering at the inlet are allowed to escape the VSA system.

In this specific model the feed column remanent fraction, η_{feed} , represents the fraction of input radon atoms being trapped in the feed column of the VSA. After the n^{th} feed of the VSA,

$$(N_{out})_n = (N_{in})_n(1 - \eta_{feed})r_{out}, \quad (4.1a)$$

and

$$(N_{in})_{n+1} = N_{det} + (N_{in})_n(1 - \eta_{feed})r_{purge} + (N_{in})_n\eta_{feed}e^{-\frac{t_{feed}}{\tau}}, \quad (4.1b)$$

where the last term represents the number of radon atoms that did not decay in the column during the feed stage; t_{feed} is the time that a VSA column is in the feed stage, which must be less than the breakthrough time, t_b , of the column to minimize radon atoms escaping from that column; N_{in} is the number of radon atoms that enter the feed column, which includes both the constant supply from the detector, N_{det} , as well as the radon atoms from the feedback loop. Note that the second term in Eq. (4.1b) represents the radon atoms that escaped the feed column and are reintroduced into the purge column by the purging gas; $r_{out} = 1 - r_{purge}$ is the fraction of the radon-reduced carrier gas that flows out of the feed column and back to the TPC detector; r_{purge} is the fraction of the radon-reduced carrier gas that is used for purging the radon-enhanced purge column.

Given the $\mathcal{O}(10 \text{ mbar})$ pressure in the purge column, the breakthrough time of the purge column is much shorter than the breakthrough time of the feed column [10]. For simplicity, the decay of radon atoms in the purge column is therefore neglected. Here the performance of Saratech charcoal is used, whose elution curve for radon in xenon carrier gas lacks significant tails in the front

or the back and is much narrower than other charcoals. The elution curve for a 50 g trap with a 200 min breakthrough time is fully contained within 100 min, or 50%, of the mean breakthrough time [2]. By increasing the trap size to 20 kg, the smallest of the column sizes discussed here, while maintaining the same aspect ratio and the same 200 min breakthrough time, the gas velocity v increases by a factor of 7.4⁵ and the longitudinal diffusion, which scales as $\sqrt{v^{-1}}$ [11], will decrease by a factor of 2.7. Therefore it is expected that, for a 20 kg trap, the radon will transit within about 20% of the breakthrough time. For a 100 kg trap, the radon transit time will be about 15% of the breakthrough time. For this reason, these traps have breakthrough times only 50% longer than the feed cycle time, yet negligible breakthrough is expected. Similarly, during the purge stage the breakthrough time is only 15% of the feed cycle time so it is assumed that no radon atoms remain in the column by the end of the purge cycle.

To make it explicit that the performance of such a RRS does not depend on the number of radon atoms supplied by the detector, we estimate its performance by computing the steady-state output radon fraction, $(\gamma_{out})_{ss} = (N_{out})_{ss}/N_{det}$ for various values of parameters η_{feed} , r_{purge} , and t_{feed} . The evolution of radon fractions obtained from Eqs. (4.1a) and (4.1b) becomes

$$(\gamma_{out})_n = (\gamma_{in})_n(1 - \eta_{feed})r_{out}, \quad (4.2a)$$

$$(\gamma_{in})_{n+1} = 1 + (\gamma_{in})_n(1 - \eta_{feed})r_{purge} + (\gamma_{in})_n\eta_{feed}e^{-\frac{t_{feed}}{\tau}}. \quad (4.2b)$$

As an example, the left panel of Fig. 9 illustrates the steady-state output radon fraction, $(\gamma_{out})_{ss}$, for VSA remanent fractions of 99%⁶, 95%, 90% with a 10% purge flow fraction in the range of feed cycle times 30 min to 600 min. The right panel of Fig. 9 demonstrates that up to 300 feed cycles are necessary to reach steady state, $(\gamma_{out})_{ss} = 0.55$, for a feed cycle time of 60 min. Details for why a 60 min feed cycle time is used for the VSA models are discussed in Appendix B. Although not explicitly shown here, fewer feed cycles are needed to reach steady state as the feed cycle times get longer. In order to increase steady state radon reduction efficacy in a VSA system, defined as $\epsilon_{RRS} = 1 - \gamma_{ss}$, one can increase the feed cycle time. This requires very large charcoal columns, since the breakthrough time, which must be larger than the feed cycle time, grows linearly with charcoal mass. It is further exacerbated in xenon-based TPC detectors because the radon adsorption coefficient k_a in xenon carrier gas (500 l/kg) is about ten times smaller than in air or even in argon carrier gas (5,400 l/kg) [2]. This does not only increase the cost associated with the increased trap size, but also the amount of xenon stored in the charcoal, which is about 0.4 kg/kg at room temperature and 1 atm [2], and can become a significant fraction of the entire xenon mass.

Note that the assumption of a feed column with remanent fraction of 99% may be optimistic. Relaxing that number to 90% will increase the steady state output radon fraction from 55% to 93%. This relaxation may be necessary for charcoal beds where long, non-Gaussian tails at the front of their elution curves provide significant radon leakage even for feed cycle times much shorter than

⁵In order to maintain the same breakthrough time, the carrier gas velocity must scale with the column length which, with a constant length/diameter ratio, increases as the cube root of the mass. The carrier gas velocity of a 20 kg trap compared to a 50 g trap then scales by $\left(\frac{20,000g}{50g}\right)^{1/3} = 7.4$.

⁶For a feed column with remanent fraction of 99%, 1% of the radon atoms entering the column are allowed to escape it, while the other 99% remain in the column during the feed cycle.

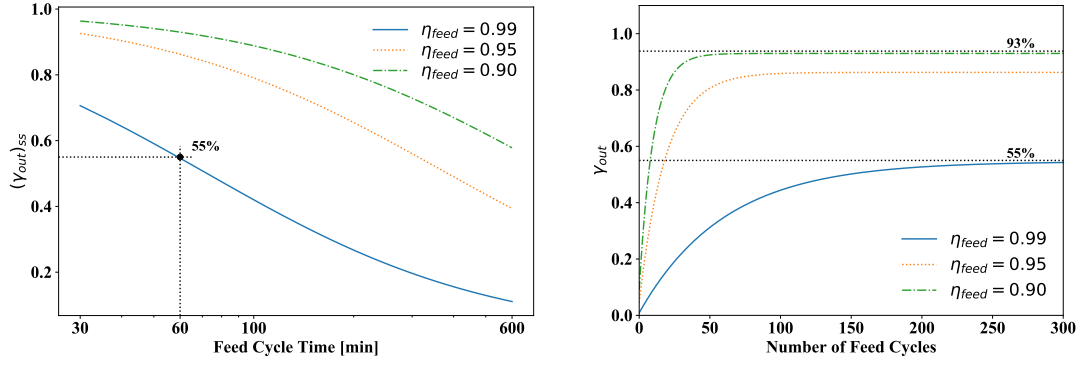


Figure 9. Dynamics of radon atoms in a VSA system with 10% purge flow fraction in the feedback loop for feed column remanent fractions of 99%, 95%, and 90%. The intrinsic activity of charcoal is ignored in this computation. Left panel: steady state fraction of radon atoms escaping the VSA versus feed cycle times for xenon purification in 30 – 600 min range. Right panel: fraction of radon atoms escaping the trap versus the number of feed cycles for a feed cycle time of 60 min and three feed column remanent fractions. As indicated with the horizontal dotted lines, it takes about 300 (60) feed cycles to approach a steady state output radon fraction of 55% (93%) in the VSA with feed column remanent fractions of 99% (90%).

the mean breakthrough time. As described in Sec. 4.1.1, this can be avoided by careful selection of the charcoal, and is less significant with larger charcoal columns.

4.1.2 Adding a cold single trap to the Feedback Loop

An improvement is to integrate a single-trap RRS, which is preferably cooled, in the feedback loop of the VSA system, shown schematically in Fig. 10, such that the radon-enhanced gas from the purge column passes through the single-trap RRS before it is fed back into the inlet of the VSA. Such a trap provides a space for radon atoms to decay before being returned to the VSA. In such a system, only a small fraction (say 10%) of the entire carrier gas circulation volume has to pass through the single-trap RRS. In addition, we will show that this trap can have a relatively low efficacy while still significantly improving the performance of the system.

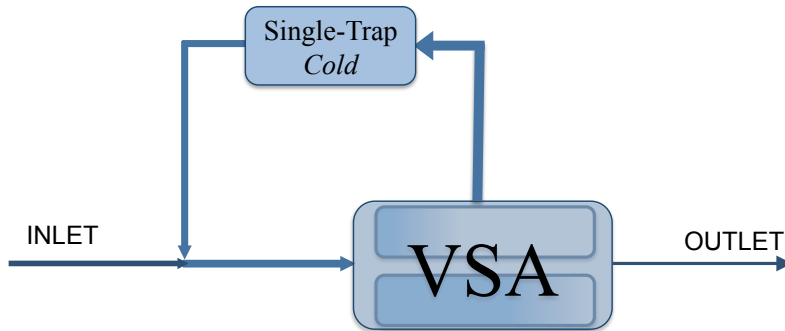


Figure 10. A schematic of a VSA system with a single, cold trap in the feedback loop for radon reduction in xenon. The cold trap greatly enhances the efficacy of the VSA system.

The addition of a single-trap in the VSA feedback loop can be implemented in the radon dynamics

model with a small modification in Eq. (4.2b), so that

$$(\gamma_{in})_{n+1} = 1 + (1 - \varepsilon_{st}) \left[(\gamma_{in})_n (1 - \eta_{feed}) r_{purge} + (\gamma_{in})_n \eta_{feed} e^{-\frac{t_{feed}}{\tau}} \right]. \quad (4.3)$$

where ε_{st} is the efficacy of the single trap. The inclusion of this trap also smooths out variations in radon concentration, which would otherwise be greater at the beginning of the cycle than at the end, justifying the approximation that η_{feed} is constant over the course of a cycle.

For illustration purposes, let us continue with the example from Sec. 4.1.1. We still neglect the intrinsic activity of the charcoal, and we still assume the VSA feed cycle time is 60 min, and the purge flow fraction to be 10%. But now we integrate a single-trap with a modest efficacy of 10% in the feedback loop of the VSA with a feed column remanent fraction of 90%. The result of such an arrangement is shown as dotted white lines in Fig. 11, which depicts a map of the RRS efficacy as a function of single-trap efficacy and feed column remanent fraction. A steady state RRS efficacy of 52% is reached. This corresponds to a reduction in the steady state output radon fraction of almost a factor of two over a VSA system without a single-trap of modest efficacy (see Fig. 9 for comparison).

Thus it appears that introducing a single trap, even with modest efficacy, in the feedback loop of a VSA system seems feasible, if the intrinsic radon activity of the activated charcoal can be ignored. Details for how to design a single trap with 10% efficacy in a feedback loop are discussed in Appendix A.

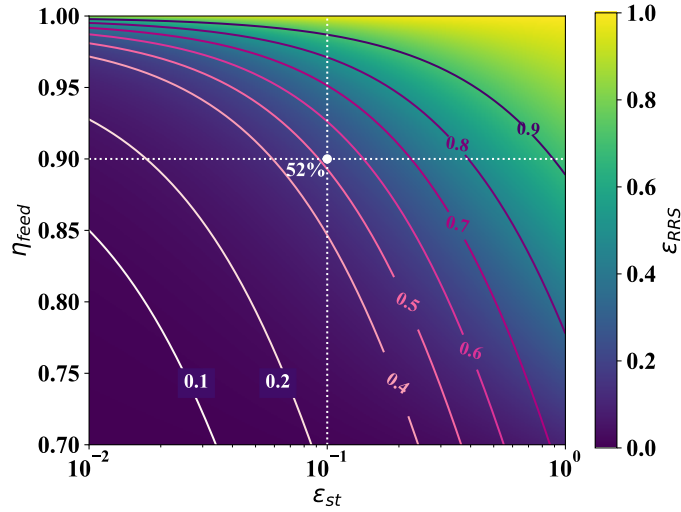


Figure 11. Radon reduction efficacy as a function of single-trap efficacy, ε_{st} , and VSA feed column remanent fraction, η_{feed} , assuming a VSA feed cycle time of 60 min and a purge flow fraction of 10%, but ignoring the intrinsic radon activity introduced by the trap. The efficacy is independent of the number of inlet radon atoms from the detector and does not have an explicit dependence on the detector parameters or the adsorptive properties of the trap. The white point indicates about 52% radon reduction efficacy as a result of a single-trap with 10% efficacy in the feedback loop of a feed column with remanent fraction of 90%.

Based on Eq. (2.9) in Sec. (2), radon reduction within a TPC detector, such as LZ, can be computed for a given efficacy of the RRS and detector volume-exchange time. For the 52% efficacy considered in the example, the radon reduction efficacy within LZ ($F = 500 \text{ SLPM}$ and

$M = 10,000\text{kg}$) is calculated to be 55%, which is close to the maximal 70% achievable with a perfect RRS system. Combining the Fig. 11 results with Eq. (2.9), the steady state radon reduction performance in the LZ detector with a swing adsorption RRS in the main circulation path, as a function of the single trap efficacy, ε_{st} and VSA feed remanent fraction, η_{feed} is shown in Fig. 12.

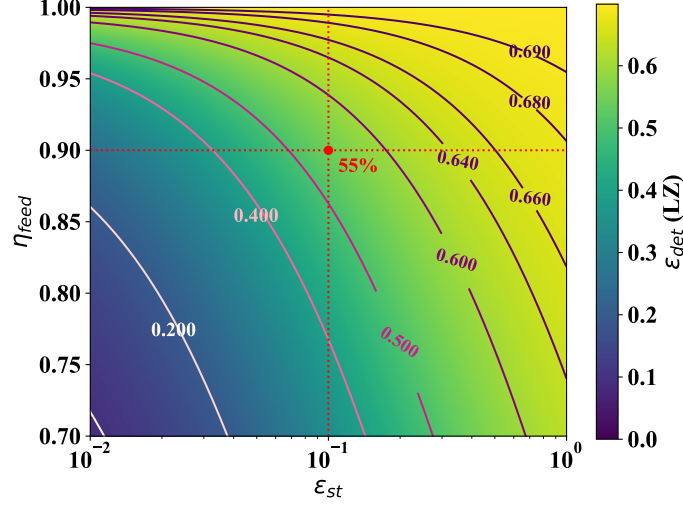


Figure 12. Steady state radon reduction efficacy in the TPC detector such as LZ ($F = 500\text{SLPM}$ and $M = 10,000\text{kg}$) with a swing adsorption RRS in the main circulation path, as a function of single-trap efficacy, ε_{st} , and VSA feed column remanent fraction, η_{feed} , assuming a VSA feed cycle time of 60 min and a purge flow fraction of 10%. The efficacy is independent of the number of inlet radon atoms from the detector, and does not have explicit dependence on the detector parameters or adsorptive properties of the trap. The red point indicates about 55% radon reduction in the TPC detector with a RRS efficacy of 52%.

4.1.3 Swing Adsorption RRS with non-zero Intrinsic Activity

Radon levels desired in a dark matter detector $\mathcal{O}(1\mu\text{Bq/kg})$ are about 5 orders of magnitude lower than those required in radon-reduced clean-rooms $\mathcal{O}(100\text{mBq/kg})$. It is therefore not realistic to assume that the intrinsic activity of the charcoal can be ignored. In Eqs. (4.2a) and (4.3), which describe the evolution of radon fractions in an adsorption swing system, γ_{in} and γ_{out} correspond to the input and output radon fractions in a single feed cycle. Thus we need to find the fraction $\gamma_{col} = N_{col}/N_{det}$, where N_{col} is the number of radon atoms introduced to the VSA due to emanation from a charcoal column in one feed cycle, and N_{det} is the number of detector radon atoms per feed cycle. N_{col} and N_{det} are independent quantities and need to be calculated separately.

The total radon activity of a charcoal column (referred to as trap in Sec. (3)), A_{col} , with breakthrough time t_b , is given by Eq. (3.6), which is the steady state radon contribution taking into account self adsorption of radon atoms that have been emanated deeper in the col. However the number of radon atoms introduced to the VSA by a col is not a steady state contribution since the flow through a VSA column is not continuous. The radon contribution from a column in a feed cycle can be expressed as

$$N_{col} = \int_0^{t_{feed}} dt \int_0^{t_b} dt' \frac{s_o m}{t_b} e^{-\frac{t'}{\tau}} H(t-t') = \int_0^{t_{feed}} dt \int_0^t dt' \frac{s_o m}{t_b} e^{-\frac{t'}{\tau}}, \quad (4.4)$$

where $H(t - t')$ is the Heaviside step function. This includes only the radon contribution from the part of the trap that had enough time to reach the outlet. Therefore a column contribution in a single feed cycle is obtained from Eq. (4.4) to be

$$N_{col} = \tau^2 \frac{s_o m}{t_b} \left[e^{-\frac{t_{feed}}{\tau}} - \left(1 - \frac{t_{feed}}{\tau} \right) \right], \quad (4.5)$$

which can be approximated to

$$N_{col} \approx \frac{s_o m}{2 t_b} t_{feed}^2. \quad (4.6)$$

This approximation is valid since the feed cycle time of the VSA is much shorter than the radon lifetime ($t_{feed} \ll \tau$), and because by ignoring the radon decay term it will always over-estimate radon content.

For calculating N_{det} , care needs to be taken to estimate the number of inlet radon atoms in a single feed cycle, since the RRS efficacy will depend on it. The number of input radon atoms in one feed cycle time is

$$N_{det} = \rho c_{Rn} F t_{feed} \tau, \quad (4.7)$$

where ρ is the density of the carrier gas at STP, c_{Rn} is the radon concentration in the carrier gas, F is the carrier gas circulation flow rate, and t_{feed} is the feed cycle time.

We can now estimate the total efficacy of a RRS considering non-zero intrinsic charcoal activity by including the fractional radon contribution from the VSA columns, $\gamma_{col} = N_{col}/N_{det}$. Using Eq. (3.1), (4.6), and (4.7), the fractional radon contribution from a VSA column per feed cycle time can be expressed as

$$\gamma_{col} = \frac{N_{col}}{N_{det}} = \frac{1}{2} \left(\frac{1}{\rho k_a} \right) \left(\frac{s_o}{c_{Rn}} \right) \left(\frac{t_{feed}}{\tau} \right) \left(\frac{f_{col}}{F} \right), \quad (4.8)$$

where f_{col} is the volumetric flow rate of the carrier gas through the VSA column (for either feed or purge). For the feed column, $f_{feed}/F = 1/r_{out}$, so that

$$\gamma_{feed} = \frac{1}{2} \left(\frac{1}{\rho k_a} \right) \left(\frac{s_o}{c_{Rn}} \right) \left(\frac{t_{feed}}{\tau} \right) \left(\frac{1}{r_{out}} \right). \quad (4.9)$$

For a purge fraction of 10%, the radon breakthrough time in the feed column is about an order of magnitude greater than the breakthrough time in the purge column. The mass flow rate of the purge flow is (1/10) of the feed flow, but the purge pressure is (1/100) of the feed pressure, resulting into a 10 times larger volumetric flow rate ($f \propto \phi/P$, where ϕ is the mass flow rate, f is the volumetric flow rate and P is the pressure) [4]. Thus, the volumetric flow rate of the purge flow is 10 times faster than that of the feed flow, that is

$$\gamma_{purge} = 10 \gamma_{feed}. \quad (4.10)$$

The fractional radon contributions expressed in Eqs. (4.9) and (4.10) can be added to Eqs. (4.2a) and Eq. (4.3) such that

$$(\gamma_{out})_n = (\gamma_{in})_n (1 - \eta_{feed}) r_{out} + \gamma_{feed} r_{out}, \quad (4.11a)$$

and

$$\begin{aligned}
 (\gamma_{in})_{n+1} = 1 + (1 - \epsilon_{st}) & \left[(\gamma_{in})_n (1 - \eta_{feed}) r_{purge} \right. \\
 & + (\gamma_{in})_n \eta_{feed} e^{-\frac{t_{feed}}{\tau}} \\
 & \left. + \gamma_{feed} r_{purge} + \gamma_{purge} \right].
 \end{aligned} \tag{4.11b}$$

The second term of Eq. (4.11a), $\gamma_{feed} r_{out}$, represents the fraction of radon atoms emanated from the charcoal in the feed column that flow into the TPC detector. In the last line of Eq. (4.11b), $\gamma_{feed} r_{purge}$ represents the fraction of radon atoms introduced by the purge flow from the feed column, and γ_{purge} represents the radon contribution due to emanation in the purge column.

The evolution of radon fractions for non-negligible intrinsic radon activity of charcoal is governed by Eqs. (4.11a) and (4.11b), and the output radon fraction depends on the ratio of intrinsic activity of the charcoal and radon concentration in the carrier gas, s_o/c_{Rn} .

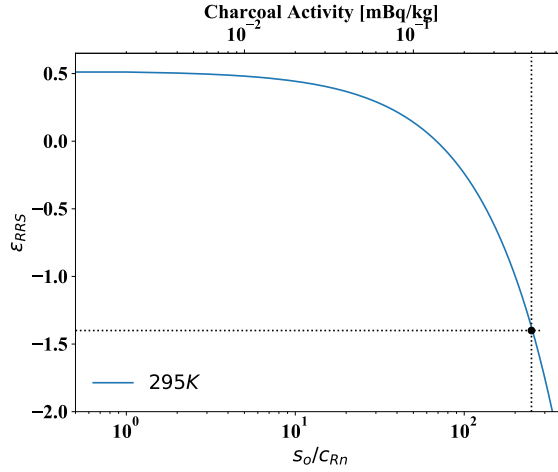


Figure 13. Efficacy of a swing adsorption RRS as a function of s_o/c_{Rn} , the ratio of intrinsic charcoal activity to inlet radon concentration. The parameters used here are $\epsilon_{st} = 0.1$, $\eta_{feed} = 0.9$, and $r_{purge} = 0.1$. The feed cycle time is $t_{feed} = 60$ min. The blue solid curve is at a VSA operational temperature of 295 K ($k_a = 500\text{ l/kg}$). The top axis shows the specific charcoal activity assuming an inlet radon activity of $2\text{ }\mu\text{Bq/kg}$, which is expected in the LZ detector.

Let us continue with the example illustrated in Sec. 4.1.1, where we integrated a single-trap with 10% efficacy in the feedback loop of a VSA with a feed column that has a 90% remanent fraction, assuming a VSA feed cycle time of 60 min and a purge flow fraction of 10%. We can now estimate the total efficacy of the RRS considering non-zero intrinsic charcoal activity. In this case, the fractional radon contribution from the VSA columns, given by Eq. (4.8), makes the RRS efficacy dependent on the charcoal adsorption coefficient. Figure 13 shows the efficacy of a VSA at room temperature (295 K , and $k_a = 500\text{ l/kg}$) as a function of s_o/c_{Rn} , the ratio of intrinsic charcoal activity to inlet radon concentration. The density at STP of xenon is taken as $\rho = 5.86\text{ g/l}$. The dotted black lines indicate that an RRS with a charcoal activity of 0.5 mBq/kg (ie. lowest currently available activity of Saratech charcoal), and a $2\text{ }\mu\text{Bq/kg}$ radon concentration in the inlet xenon would be quite harmful, because it would introduce considerably more radon than it removes. It

would require a charcoal with the same adsorption properties as Saratech, but with about an order of magnitude lower activity, to be effective at room temperature.

4.1.4 Operating a cold Swing Adsorption RRS

Up to now, VSA operation has only been considered at room temperature. However, because the adsorption coefficient of charcoal increases with decreasing temperature following the Arrhenius Law [2] (ie. from $k_a = 500 \text{ l/kg}$ at 295 K to $k_a = 3,000 \text{ l/kg}$ at 190 K), cooling the VSA down to 190 K shows considerable promise, particularly at higher s_o/c_{Rn} ratios. The efficacy of the cooled VSA system becomes comparable to that of a VSA system operated at room temperature, but with significant relaxation on the demand for intrinsic charcoal activity as seen in Fig. 14. In fact, the demand relaxes by about an order of magnitude, which may be in reach by the time future generation experiments can be realized [12].

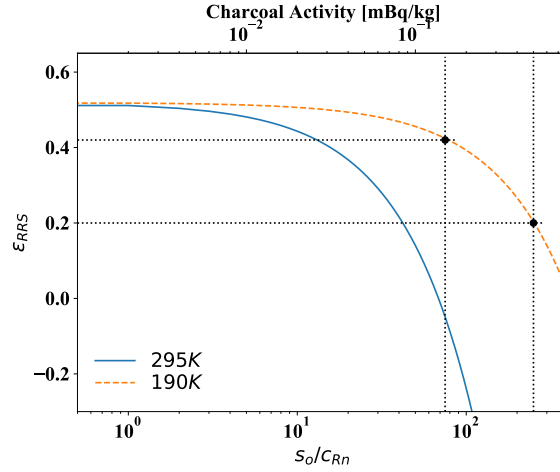


Figure 14. Efficacy of a swing adsorption RRS as a function of s_o/c , the ratio of intrinsic charcoal activity to inlet radon concentration. The parameters used here are $\epsilon_{st} = 0.1$, $\eta_{feed} = 0.9$, and $r_{purge} = 0.1$, and the feed cycle time is $t_{feed} = 60 \text{ min}$. The dashed orange curve represents the efficacy of the RRS when the VSA is cooled down to 190 K ($k_a = 3,000 \text{ l/kg}$), and the blue solid curve is at a VSA operational temperature of 295 K ($k_a = 500 \text{ l/kg}$). The top axis shows the specific charcoal activity, assuming an inlet radon activity of $2 \mu\text{Bq/kg}$, which is expected in the LZ detector. The two sets of dotted black lines show that the best RRS efficacy with currently available charcoal is about 20%, and that about a factor of 3 lower specific charcoal activity is needed to reach a factor of 2 radon reduction in the LZ detector, if the VSA is cooled down to 190 K . If the VSA was operated at room temperature, however, about a factor of 20 lower specific charcoal activity would be needed to reach a factor of 2 radon reduction in the LZ detector. That appears out of reach in time for the next generation of experiments.

Specifically, for an inlet radon concentration of $2 \mu\text{Bq/kg}$, expected in the LZ detector, and intrinsic charcoal activity of Saratech, 0.5 mBq/kg , a cold VSA would have about 20% efficacy. This is in stark contrast to a VSA operated at room temperature, which is very harmful, as discussed in Sec. 4.1.3. In order for such a RRS to reach 42% efficacy for an inlet radon activity of $2 \mu\text{Bq/kg}$, charcoal with intrinsic activity of 0.16 mBq/kg (about a factor of 3 lower than that of Saratech) is necessary. Note that 42% RRS efficacy corresponds to a factor of 2 radon reduction in the LZ detector (see Fig. 2).

5. Conclusion

Radon and its daughters constitute the most significant backgrounds in rare event searches since they are continuously resupplied from detector materials. Although radon screening of every single detector component is vital to reach high sensitivity for dark matter detection, it is not sufficient. Further mitigation strategies are required that include both, in-situ hardware radon reduction and background discrimination in the analysis of the data.

The performance of charcoal-based radon reduction systems has been explored. For illustration purposes, references to the LZ detector have been made, but the general arguments and observations are not limited to one specific dark matter experiment. In-line radon reduction systems in auxiliary circulation loops, as employed in the LZ experiment, reduce radon-rich gaseous xenon from the warm components of the detector before they return radon-reduced xenon back to the main circulation loop. This single, charcoal-based, adsorption trap approach is effective for slow circulation flow rates, but breaks down at high circulation flow rates, which are required to purify entire volumes of ton scale or larger noble-liquid detectors. It is found that scaling up charcoal-based single-trap radon reduction systems to make them viable at the circulation flow rates of multi-ton TPC detectors is impractical even if radon emanation from charcoal is negligible.

Vacuum swing adsorption systems, which have shown great success at reducing atmospheric radon levels in clean-rooms, have clear advantages over single-trap systems. However, they need to be modified so that they can capture and return the noble carrier gases to the purification system through a gas feedback loop rather than releasing them into the atmosphere. The drawback of such systems is that the radon atoms become effectively trapped and can lead to many-fold higher radon concentrations in the feedback circulation loop. This can be ameliorated by introducing a modest cold single-trap into the feedback loop. It allows the radon atoms to accumulate and decay in the single trap, rather than in the charcoal columns of the swing adsorption system, where some fraction can escape and be reintroduced into the TPC detector. It is found that for a VSA system with a feed column of 90% remanent fraction, introduction of even a 10% efficacy single trap in the feedback loop reduces the steady state output radon fraction from about 90% to about 50%.

While this is encouraging, it needs to be pointed out that VSA systems too are limited by the intrinsic radon activity of their charcoal adsorbent, particularly if they are operated at room temperature. Under these circumstances, adsorbents with about a factor of 20 lower intrinsic radon activity than in currently available activated charcoals are required to build effective vacuum swing adsorption systems for rare event search experiments. If such VSA systems are instead cooled to about 190K, this factor drops from 20 to about 3, which may be in reach by the time future generation experiments can be realized. Other options, not pursued here, might include radon purification in the liquid phase.

Acknowledgments

We acknowledge support of the U.S. Department of Energy (DOE) Office of Science under grant numbers DE-SC0015708 and DE-SC0019193, and under contract number DE-AC02-76SF00515, the SLAC National Accelerator Laboratory and the University of Michigan. We would like to thank

Dr. Richard Raymond at the University of Michigan for many helpful conversations. We would also like to thank the members of the LZ collaboration for many insightful discussions.

A. A closer look at the single-trap in the Feedback Loop

The example of a VSA system with 90% remanent fraction, discussed in Sec. 4.1.2, included a single-trap in the feedback loop. It was assumed that this single trap had a modest efficacy of 10%. For a purge fraction of $f_{\text{purge}} = 0.1$, a detector such as the LZ detector (500 *SLPM*) would need to support a 50 *SLPM* flow rate in the feedback loop. It is important to note that the efficacy of a single-trap depends on several parameters, which include not only the flow rate of the carrier gas, but also the specific activity of the charcoal used in the trap, and the radon activity at the input of the trap. These parameters have been explored in Sec. 3 to determine the efficacy of a standalone single-trap RRS. Equation (3.8) of Sec. 3 needs to be modified to account for the input and output radon activities in a single feed cycle. Therefore, the total single-trap contribution A_{trap} from the charcoal, introduced by the second term in Eq. (3.7a), is reduced to a contribution in a single feed cycle given by a modified version of Eq. (4.4), such that

$$\begin{aligned} (N_{\text{trap}})_{\text{feed}} &= \int_0^{t_{\text{feed}}} dt \int_0^{t_b} dt' \frac{S_o m}{t_b} e^{-\frac{t'}{\tau}} H(t_{\text{feed}} - t') = \int_0^{t_{\text{feed}}} dt \int_0^{t_{\text{feed}}} dt' \frac{S_o m}{t_b} e^{-\frac{t'}{\tau}} \\ &= t_{\text{feed}} \tau \frac{S_o m}{t_b} \left(1 - e^{-\frac{t_{\text{feed}}}{\tau}}\right) = t_{\text{feed}} A_{\text{trap}}. \end{aligned} \quad (\text{A.1})$$

Here, A_{trap} is the total contribution from a single trap given by Equation (3.6) in Sec. 3. The contribution of a single trap in a feed cycle is therefore

$$(A_{\text{trap}})_{\text{feed}} = \frac{(N_{\text{trap}})_{\text{feed}}}{\tau} = \frac{t_{\text{feed}} A_{\text{trap}}}{\tau}. \quad (\text{A.2})$$

After this modification, the efficacy of a single trap becomes

$$\varepsilon = 1 - A_{\text{out}}/A_{\text{in}} = 1 - e^{-\frac{m}{\mu}} - \frac{S_o \mu}{A_{\text{in}}} \left(\frac{t_{\text{feed}}}{\tau}\right) \left(1 - e^{-\frac{m}{\mu}}\right) = \left[1 - \frac{S_o f t_{\text{feed}}}{k_a A_{\text{in}}}\right] \left(1 - e^{-\frac{m k_a}{f \tau}}\right), \quad (\text{A.3})$$

where A_{in} is the inlet radon activity of the single-trap in the RRS feedback loop. It can be obtained from Eq. (4.11b) of Sec. 4.1.3 by noting that $(\gamma_{\text{in}})_{n+1} = 1 + (\gamma_{\text{loop}})_n$, such that the radon fraction in the feedback loop is given by

$$\begin{aligned} (\gamma_{\text{loop}})_n &= (1 - \varepsilon_{\text{st}}) \left[(\gamma_{\text{in}})_n (1 - \eta_{\text{feed}}) r_{\text{purge}} \right. \\ &\quad \left. + (\gamma_{\text{in}})_n \eta_{\text{feed}} e^{-\frac{t_{\text{feed}}}{\tau}} \right. \\ &\quad \left. + \gamma_{\text{feed}} r_{\text{purge}} + \gamma_{\text{purge}} \right]. \end{aligned} \quad (\text{A.4})$$

For a N_{det} radon input from the detector in one feed cycle, defined by Eq.(4.7), the single trap inlet radon activity in a feed cycle becomes

$$A_{\text{loop}} = N_{\text{det}} \gamma_{\text{loop}} / \tau. \quad (\text{A.5})$$

At steady state, which is reached in about 30 feed cycles with a cold VSA ($k_a = 3,000 \text{ l/kg}$ at 190 K), $A_{\text{loop}} = 2.55 \text{ mBq}$, as shown in left panel of Fig. 15. The parameters used here are $\varepsilon_{\text{st}} = 0.1$,

$\eta_{feed} = 0.9$, $r_{purge} = 0.1$, $c_{Rn} = 2 \mu\text{Bq/kg}$, and $s_o = 0.5 \text{ mBq/kg}$. The feed cycle time is $t_{feed} = 60 \text{ min}$. A general feature of RRS efficacy is that the higher the single-trap efficacy the fewer feed cycles are needed to reach steady state, while the higher the feed column efficacy the larger the number of feed cycles are needed. The right panel of Fig. 15 shows the efficacy of a single-trap ($k_a = 3,000 \text{ l/kg}$ at 190 K) as a function of charcoal mass, for a range of intrinsic charcoal activities at a fixed flow rate of 50 SLPM . It indicates that about 18 kg of charcoal with an intrinsic activity of $s_o = 0.5 \text{ mBq/kg}$ is needed to reach a 10% efficacy. Note that building a single-trap with an efficacy near 10% is not very sensitive to the intrinsic activity of the charcoal.

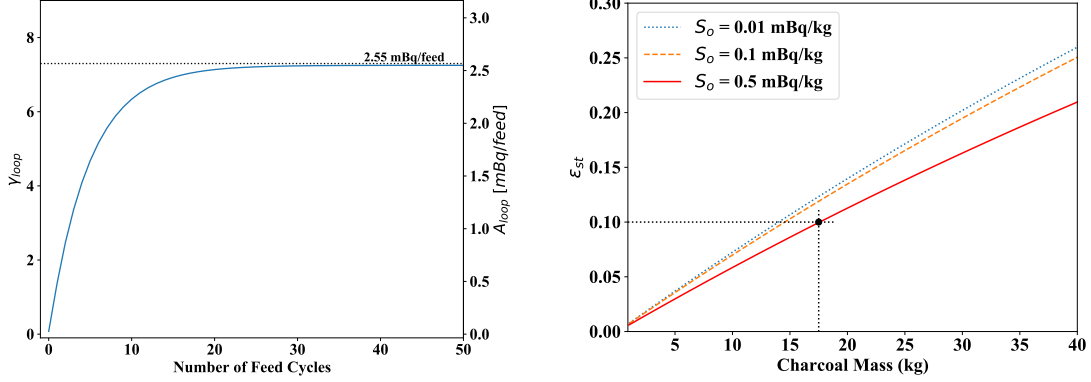


Figure 15. Left panel: Evolution of radon activity in the VSA feedback loop as a function of feed cycles. Steady state is reached after about 30 feed cycles with a cooled down VSA ($k_a = 3,000 \text{ l/kg}$ at 190 K). The steady state radon activity in the loop is 2.55 mBq per feed cycle, which is about 7.3 times greater than the radon activity provided by the TPC detector, indicated by the dotted black line. The parameters used here are $\epsilon_{st} = 0.1$, $\eta_{feed} = 0.9$, $r_{purge} = 0.1$, $c_{Rn} = 2 \mu\text{Bq/kg}$, and $s_o = 0.5 \text{ mBq/kg}$. The feed cycle time is $t_{feed} = 60 \text{ min}$. Right panel: Radon reduction efficacy of a single-trap with dynamic adsorption coefficients of $k_a = 3,000 \text{ l/kg}$ and an inlet radon activity of $A_{loop} = 2.55 \text{ mBq}$ are shown as a function of charcoal mass for various intrinsic radon activities. The dotted black lines indicate that about 18 kg of charcoal with intrinsic activity of $s_o = 0.5 \text{ mBq/kg}$ will give a single-trap with 10% efficacy in the feedback loop of the swing system.

B. Considerations for the Feed Cycle Time in a Swing Adsorption RRS

Throughout this document we have used a feed cycle time of 60 min as an example; however, this choice is not without consequence. As shown in Fig. 16, the number of radon atoms escaping $(\gamma_{out})_{ss}$ from a VSA with a single-trap in its feedback loop does depend on the feed cycle time, even when other properties of the individual traps (ie. the mass) are adjusted to obtain the same performance of $\eta_{feed} = 0.9$. When there is no radon emanation from the charcoal (ie. $s_o = 0$), then a longer feed cycle time is advantageous – radon atoms captured in the VSA’s feedback loop have a 10% chance to escape each cycle, so a longer feed cycle time provides them fewer opportunities before their eventual decay. Conversely, in the realistic case where there *is* emanation from the charcoal, then a shorter feed cycle time is preferable. This is a consequence of the highly-effective purge cycle leaving the column free of radon. Atoms emanated must transit to the trap’s exit within the feed cycle time in order to contribute to the concentration at the system output, so the emanation

contribution is proportional to t_{feed}^2 . This is derived in Eqs. (4.5-4.9), and appears as a linear slope of $(\gamma_{out})_{ss}$ in Fig. 16.

While a shorter feed cycle time is advantageous in a system dominated by charcoal emanation, it is technically challenging to implement a system with an arbitrarily small feed cycle time. Any real system will require some finite time to evacuate the column, bringing it from forward flow pressure to purge cycle pressure, during which time the purge cycle is ineffective. In practice this means $t_{purge} = t_{feed} - t_{pump}$, so the statement that $t_{purge} = t_{feed}$ is only true when $t_{feed} \gg t_{pump}$. Typical VSA systems in air require tens of seconds to pump out, so this condition is achieved with feed cycle times of approximately one hour or longer. Thus, a feed cycle time of one hour was used for the calculations in this paper.

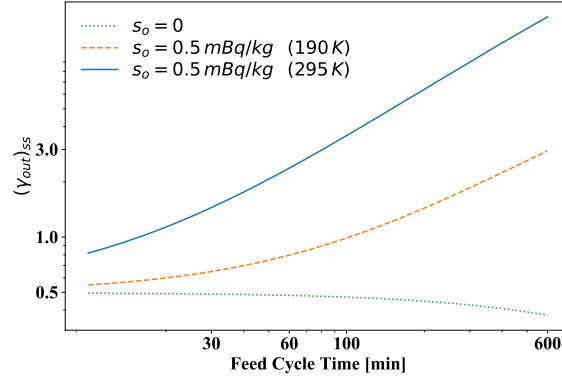


Figure 16. Steady state fraction of radon atoms escaping the RRS versus feed cycle times for xenon purification in 10 – 600 min range. The parameters used are $\epsilon_{st} = 0.1$, $\eta_{feed} = 0.9$, and $r_{purge} = 0.1$. The dotted green curve is for the case of no intrinsic charcoal activity and is independent of inlet radon activity, while the dashed orange and the solid blue curves assume $c_{Rn} = 2 \mu\text{Bq/kg}$ and $s_o = 0.5 \text{ mBq/kg}$. The orange curve represents the efficacy of the RRS when the VSA is cooled down to 190 K ($k_a = 3,000 \text{ l/kg}$), and the blue curve is at a VSA operational temperature of 295 K ($k_a = 500 \text{ l/kg}$).

As discussed in Sec. 4.1.1, the tight elution curves of Saratech charcoal allow traps to have breakthrough times that are only about 50% longer than the feed cycle time, but with negligible radon breakthrough. This leads to breakthrough times of $t_b = 1.5 t_{feed} = 90 \text{ min}$, and in turn, since $t_b = k_a m / f$, to VSA columns that are of $\mathcal{O}(100 \text{ kg})$ if operated at room temperature ($k_a = 500 \text{ l/kg}$), and $\mathcal{O}(20 \text{ kg})$ if operated at 190 K ($k_a = 3,000 \text{ l/kg}$), at flow rates near $f = 500 \text{ SLPM}$.

There is one additional consideration, especially for the cold VSA discussion. In order for the purge cycle to be effective, the characteristic time that a radon atom is stuck to charcoal must be much shorter than the duration of the purge cycle. It is possible that the low temperatures discussed here will require longer swing-cycle periods as this characteristic time increases with reduced temperature.

References

- [1] LZ Collaboration, D. Akerib et al., *The LUX-ZEPLIN (LZ) Technical Design Report*, arXiv:1703.09144 [physics.ins-det]

- [2] K. Pushkin et al., *Study of radon reduction in gases for rare event search experiments*, Nucl. Instrum. Meth. **A903** (2018) 267.
- [3] XENON Collaboration, S. Moriyama et al., *Direct Dark Matter Search with XENONnT*, https://www.lowbg.org/ugnd/workshop/sympo_all/201903_Sendai/slides/8am/8am_6.pdf.
- [4] A. Pocar, *Low Background Techniques and Experimental Challenges for Borexino and its Nylon Vessels*, Ph.D. Thesis Princeton (2003), Report number: UMI-31-03047
- [5] J. Street et al., *Construction and Measurements of an Improved Vacuum-Swing-Adsorption Radon-Mitigation System*, AIP Conference Proceedings **1672**, 150004 (2015), <https://aip.scitation.org/doi/10.1063/1.4928027>.
- [6] J. Street et al., *Radon Mitigation for the SuperCDMS-SNOLAB Dark Matter Experiment*, AIP Conference Proceedings **1921**, 050002 (2018), <https://aip.scitation.org/doi/abs/10.1063/1.5018995>.
- [7] M. Arthurs, D. Huang, C. Amarasinghe, E. Miller, W. Lorenzon, <https://gitlab.com/armaris/charcoal-based-RRS-performance-study> (2020).
- [8] ICARUS collaboration, P. Benetti et al., *Argon purification in the liquid phase*, Nucl. Instrum. Meth. **A333** (1993) 567.
- [9] XMASS collaboration, A. Abe, et al., *Radon removal from gaseous xenon with activated charcoal*, Nucl. Instrum. Meth. **A661** (2012) 50.
- [10] R.W. Schnee, R. Bunker, G. Ghulam, D. Jardin, M. Kos and A.S. Tenney, *Construction and measurements of a vacuum-swing-adsorption radon-mitigation system*, <https://aip.scitation.org/doi/abs/10.1063/1.4818089>.
- [11] R.L. Grob, *Modern Practice of Gas Chromatography*, John Wiley and Sons, 2nd edition, 1985.
- [12] Private communications with Blücher GMBH, the German producer of the Saratech brand charcoal, revealed that the cleanliness of their charcoal could be significantly improved if they used their quartz glass reactor rather than their metal reactor for production.